Shadow detection for depth image of Kinect sensor based on fractional differential

Zhang Tong[1], Liu Sheng[2], Cao Ting[1]

(1. School of Computer Science and Engineering, Xi′an University of Technology, Xi′an 710048, China;
2. Faculty of Information Technology and Equipment Engineering, Xi′an University of Technology, Xi′an 710048, China)

Abstract: As an essential component of the Kinect sensor, depth image always contains inevitable and unpredictable shadow noises which limit their usability in many 3D vision applications. Therefore, a shadow detection method based on fractional differential was proposed for depth image. Based on the study of Tiansi template defined by fractional differential, a non-linear stretching operator was designed and implemented. This operator can enhance the boundaries information of shadow regions significantly and accomplish the shadow detection effectively at 0.6 order. Compared with other traditional methods, the proposed method can reach up to 0.971 for F-measure, while the other methods were all less than 0.7. The experimental results indicate that the new method can detect shadow noises effectively.

Key words: depth image; noise detection; fractional differential; shadow detection

CLC number: TP391 **Document code:** A **DOI:** 10.3788/IRLA201948.0826002

基于分数阶微分的 Kinect 传感器深度图像阴影检测方法

张 彤[1],刘 晟[2],曹 霆[1]

(1. 西安理工大学 计算机科学与工程学院,陕西 西安 710048;
2. 西安理工大学 信息技术与装备工程学院,陕西 西安 710048)

摘 要: 深度图像作为 Kinect 传感器的重要组成部分,其获得的深度图像往往伴随着不可避免和无法预知的阴影噪声,这也极大地影响并制约其在三维可视化等方面的应用及研究。因此,针对深度图像提出了一种基于分数阶微分的阴影检测方法。在研究分数阶微分定义的 Tiansi 模板基础上,设计并实现了一种非线性拉伸算子。该算子在 0.6 阶次可以增强阴影区域边界信息的同时实现阴影的有效检测。通过分析比较发现,该方法在 F 测度的评价体系中可以达到 0.971,而其他传统的检测方法均小于 0.7。实验结果证明文中提出方法可以有效实现深度图像的阴影检测。

关键词: 深度图像; 噪声检测; 分数阶微分; 阴影检测

收稿日期: 2019-03-05; **修订日期:** 2019-04-10

基金项目: 陕西省重点研发计划(2019GY-038)

作者简介: 张彤(1968-),男,副教授,主要从事模式识别及图像处理方面的研究。Email:zhangtong@xaut.edu.cn

通讯作者: 曹霆(1988-),男,讲师,博士,主要从事计算机视觉及三维图像处理方面的研究。Email:wellcaoting@163.com

0 Introduction

Depth image plays an essential role in many 3D vision applications. Among many depth captured devices, the Microsoft Kinect sensor gained great attention due to such low price and relatively high resolution[1]. The Kinect sensor is mainly composed of an infrared light projector, a depth image sensor and a color image sensor[2]. Depth image is acquired by Kinect is based on the theory of triangulation measurement process[3].

Unfortunately, the depth image often contains some noises which greatly limit usage in practice. The noises usually exhibit as black regions which often happen around object boundaries in the scene. These black regions are due to partial occlusion of the infrared light by foreground objects, leading to shadows in some background regions which are unreachable by the IR projector pattern. The referring condition will produce the shadow noises. Hence, the shadow detection for depth is vital for the Kinect applications acquisition[4-5].

Compared with the ordinary digital image processing, the depth image processing has only been aroused in recent years. Even though, many studies on depth image including filtering, enhancement, detection, segmentation, recognition and analysis have promising achievement on the foundation of previous image theory[6-7]. Since Kinect sensor always capture a paired of images including color data and depth data, Hu studied a method to detect and fill the missing data in depth image based on the color data[8]. Also, Yang proposed a depth image segmentation method according to color information[9]. Camplani worked on a method to build up a model and fill up the hole on every frame[10]. What′s more, Maimone suggested an adaptive threshold method based on the distance in reality, and the depth values under the threshold are filtered out[11]. Essmaeel introduced a novel method to reduce the noises due to the movements in scene[12].

Many researchers still face challenges to achieve stable and effective depth image. This research resolves into develop a method for shadow detection on depth image. A novel fractional differential algorithm is studied which employs a non-linear stretching coefficient based on Tiansi operator to accomplish shadow detection. The remaining part of the paper is organized as follows: Section 2 describes the methodology and an improved operator based on fractional differential is put forward for the shadow detection. Section 3 is for the experimental results, and section 4 concludes the paper.

1 Methodology

As mentioned before, the shadow noises in depth image are due to partial occlusion of the structured light by objects, leading to shadows in some background regions which are visible in the IR camera but unreachable by the IR projector pattern [13]. Accordingly, the shadow noises will produce noisy object boundary occlusions, which directly affect the accuracy of object extraction. Therefore, the shadow detection in the depth image is very critical for applications.

1.1 Traditional edge detection

Considering the shadow noises always presents as black regions which exhibit distinguish from neighborhoods on grey value level, it is reasonable to apply edge detection methods for shadow detection. As one vital part of image processing, the edge detection has been well studied for a long time. The traditional methods of the edge detection are all carried out using integer order differential processing, for example, the first order Sobel operator and the second order Laplace operator[14].

In Fig.1, although different edge operators can present image edge information respectively, none of them can distinguish the detected shadow edges effectively. These traditional operators all are very sensitive to noises and easily affected, which could not meet the application for shadow detection in the situations. Recent years, the fractional differential

theory has applied on image edge detection[15].

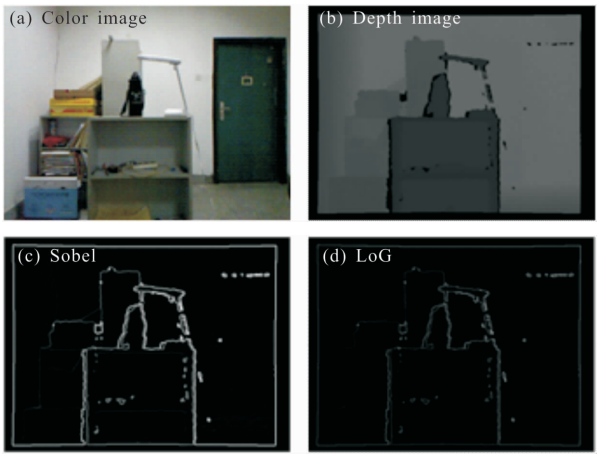

Fig.1 Depth image with integer edge detection methods

1.2 Fractional differential on signals

Fractional differentials have been used to solve problems in signal processing [16]. For an arbitrary square integrable signal $s(t) \in L^2(R)$, the $v-$order differential operator D^v is the multiplicative operator of the $v-$order differential multiplier function while $v>0$, and its $v-$order fractional differential is:

$$D^v s(t)=\frac{d^v s(t)}{dt^v} \tag{1}$$

According to the basic theory of signal processing, its Fourier transform is:

$$D^v s(t) \overset{FT}{\leftrightarrow} (\hat{D}_v s)(w)=(iw)^v s(\hat{w})=d_v(\hat{w})s(\hat{w}),\ v \in R^+ \tag{2}$$

Where $D_v=D^v$ is the $v-$order differential multipliable operator, and the filter function of fractional differential is :

$$\begin{cases} d_v(\hat{w})=(iw)^v=|w|^v \exp[i\theta_v(w)] \\ \hat{a}_v(w)=|w|^v,\ \theta_v(w)=\dfrac{v\pi}{2}\mathrm{sgn}(w) \end{cases} \tag{3}$$

Based on the above formulas, the amplitude-frequency curve can be drawn in Fig.2. We found that a fractional differential operator can increase the high frequency $1<w<2$ components of a signal. With the increasing order and frequency of fractional differential, the increasing rate shows a nonlinear rapid growth. Meanwhile, the fractional differential also preserves low frequency $0<w<1$ portion of the signal to a certain degree non-linearly. Compare with integral differentials the fractional differentials can only enhance *HF* signals and preserve *LF* signals simultaneously.

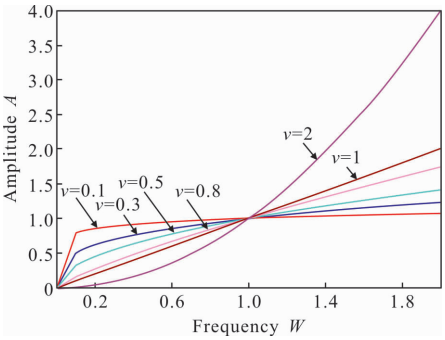

Fig.2 Amplitude-frequency curve of fractional differential

In digital image theory, the variation of gradient magnitude near the edge information is relatively high, corresponding to the high frequency components of the signal. The weak texture regions usually present intermediate frequency components and the smooth areas always exhibit *LF* portions of the signal[18].

From the first-order differential and second-order differential in Fig.2, we can infer that the operators such as Sobel ($v=1$) and Gauss-Laplace ($v=2$) are applied in image processing, the edges in the image will be enhanced, while the weak textures are will also be sharpened. However, the fractional differentials can enhance edges in an image and preserve more texture and smooth area data, making the image clearer, as show in Fig.3. Therefore, the enhancement produced by the fractional differentials is significantly better than that of integral differentials.

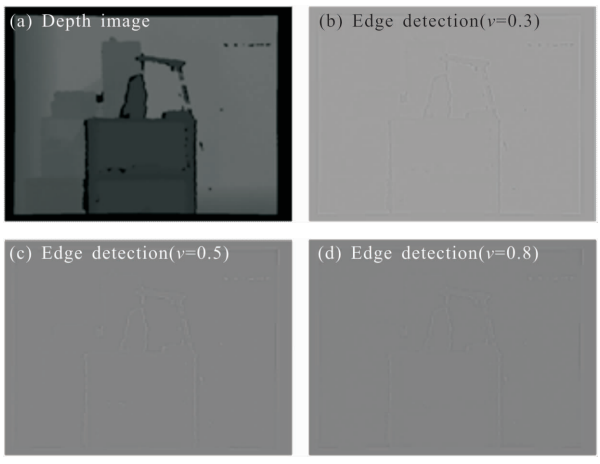

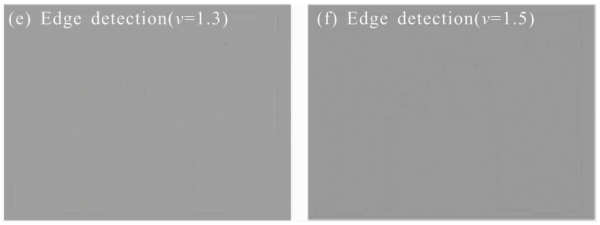

Fig.3 Fractional differential on image results with different orders

Due to the advantages mentioned before, the application of the fractional differential in image processing has aroused the attention of many researchers. However, there are still not many researchers mentioned about the shadow detection.

1.3 Improved fractional operator for shadow detection

As a theory on arbitrary order differential, the fractional differential is in accordance with integer order differential and it is the generation of the latter[19]. Researchers have given different definitions on fractional calculus from different perspectives, such as Grunwald–Letnikov (G–L), Riemann–Liouville (R–L) and Caputo. The G–L definition on fractional differential is reliable in the implementation of digital image theory[20].

For $0<v<1$, $[v]$ is the integral part of v, $f(t)\in[a,t](a,t\in R)$ is the signal with $m+1(m\in Z)$ order derivatives, then the v order derivative of $f(t)$ can be defined as:

$$ {}_{a}^{G}D_{t}^{v}f(t)\approx\lim_{\substack{h\to 0\\ n*h=t-a}}h^{-v}\sum_{r=0}^{n}\begin{bmatrix}-v\\ r\end{bmatrix}f(t-rh) \tag{4}$$

Where, $\begin{bmatrix}-v\\ r\end{bmatrix}=\dfrac{(-v)(-v+1)\cdots(-v+r-1)}{r!}$, $n=\dfrac{t-a}{h}$. So the expression of the fractional order differential is:

$$\frac{d^{v}f(t)}{\mathrm{d}t^{v}}\approx f(t)+(-v)f(t-1)+\frac{(-v)(-v+1)}{2}f(t-2)+\cdots+\frac{\Gamma(n-v-1)}{(n-1)!\ \Gamma(-v)}f(t-n+1) \tag{5}$$

For a digital image $I(x,y)$, the partial differential equation is as follows:

$$\frac{\partial^{v}I(x,y)}{\partial x^{v}}\approx I(x,y)+(-v)I(x,y-1)+\frac{(-v)(-v+1)}{2}\cdot I(x,y-2)+\cdots+\frac{\Gamma(n-v-1)}{(n-1)!\ \Gamma(-v)}I(x,y-n+1) \tag{6}$$

$$\frac{\partial^{v}I(x,y)}{\partial y^{v}}\approx I(x,y)+(-v)I(x,y-1)+\frac{(-v)(-v+1)}{2}\cdot I(x,y-2)+\cdots+\frac{\Gamma(n-v-1)}{(n-1)!\ \Gamma(-v)}I(x,y-n+1) \tag{7}$$

With rotation invariance of image template, the isotropic differential operators can be used in eight directions of the upper and lower, left and diagonal directions. The n multiplier for the difference equation can be written as:

$$a_{n}=\frac{\Gamma(n-v-1)}{(n-1)!\ \Gamma(-v)},\ n=0,1,2,\cdots \tag{8}$$

The fractional differential operator is given in Fig.4, which is known as Tiansi operator that has the nature of rotation invariance. Unfortunately, in view of the traditional G–L definition of the fractional order differential operator, although it can effectively enhance image information, it cannot meet the requirement to identify the shadows effectively.

a_2	0	a_2	0	a_2
0	a_1	a_1	a_1	0
a_2	a_1	$8\times a_0$	a_1	a_2
0	a_1	a_1	a_1	0
a_2	0	a_2	0	a_2

Fig.4 Tiansi operator

For a traditional edge detection operator, the sum of all coefficients is zero, such as Robert, Sobel and Laplace. For fractional order, the sum is not zero, which is the important distinction between integer and fractional order.

Take the 5×5 operator as an example; the sum of all items is as follow:

$$S=8a_0+8a_1+8a_2=4v^2-12v+8 \tag{9}$$

As the fractional operator, the function is $E\times A$, where, $E=1-1/S$ and A is Tiansi operator.

As we can see, when $v=1$ or $v=2$, $S=0$, and $1/S$ is none sense. So, only when v is the fractional order, $1/S$ has the mathematic meaning. This is the reason for the distinction between integer and fractional order operators.

Accordingly, set $T=S^2$ as the new sum of all items.

$$T=S^2=(4v^2-12v+8)^2 \tag{10}$$

When v is an integer order (1 or 2), S will be zero which still has the mathematic feature as mentioned E before. Moreover, as the v is a fractional order, the new function has the extraordinary result on image processing.

Finally, the result with the proposed operator is shown as:

$$I'=\left(\frac{A}{T}\otimes I\right)-I \tag{11}$$

Where, I denotes the initial image, I' presents the final image after processing, A denotes a Tiansi operator, $T=(4v^2-12v+8)^2$ and v denotes the fractional order.

As shown in Fig.5(a)-(e), the proposed operator between 0.1 and 0.6 order is more fouctional on image enhancment. While the order from 0.7 to 0.9 in Fig.5(g)-(i), it is more concentrate on image edge detection. When v=0.6, it will meet the balance of image enhancement and edge detection. It can enhance image gray level information in a nonlinear way. Also, it is able to distinguish the boundaries of shadow regions from the image.

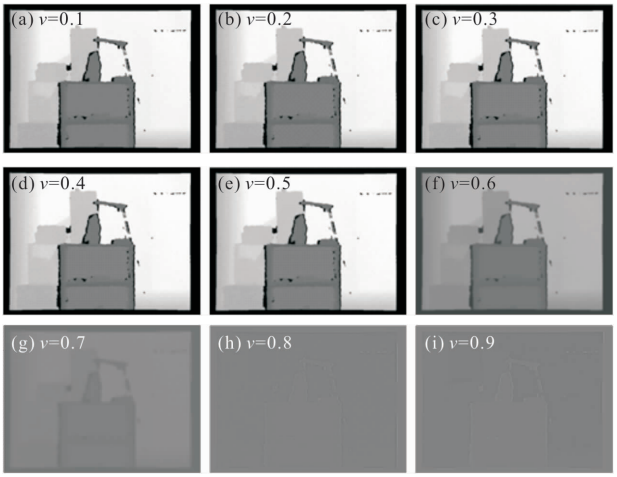

Fig.5 Different orders of proposed operator from 0.1 to 0.9

In depth image, there is not obvious difference between the shadow part and the objects. Moreover, the gray level of the shadow noises is easy to mix with the object boundaries. However, the improved fractional differential operator can nonlinearly tensile gray level and highlight the details. So, even a little distinguished gray level in a depth image can become further enlarged. Thereby, the satisfactory shadow detection can be accomplished as shown in Fig.6.

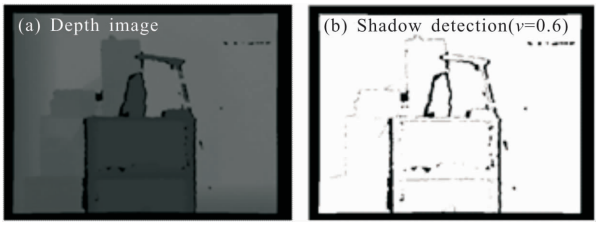

Fig.6 Proposed method on shadow detection

2 Experimental results

In this paper, the Kinect related its SDK is used to access and obtain depth image from the Kinect sensor. All of the filtering methods are implemented in Visual studio 2010 platform, and the related codes are programmed with the libraries including OpenCV, PCL and OpenNI.

To verify the performance of these algorithms mentioned above, the F-measure system[20]. including Recall, Precision and F_1-score are used to evaluate the shadow detection results. In the evaluation, the ground truth is achieved manually, which is considered as the best result. Recall describes the completeness of shadow pixels which are detected comparing with the ground truth. Precision represents the percentage of the detected pixels which are correct. F_1-score is an overall evaluation criterion based on Recall and Precision. Their formulae are as follows:

$$\begin{cases} R_e=\dfrac{L_{TP}}{L_{GT}}=\dfrac{L_{TP}}{L_{TP}+L_{FN}} \\ P_r=\dfrac{L_{TP}}{L_{TP}+L_{FP}} \\ F_1=2\dfrac{R_e\cdot P_r}{R_e+P_r} \end{cases} \tag{12}$$

Specifically, L_{TP} (True Positive) denotes the number of pixels which are detected as shadows correctly. L_{FN} (False Negative) stands for the number of shadow pixels that are undetected. L_{FP} (False

Positive) means the number of non-shadow pixels which are detected as shadows. L_{GT} (Ground Truth) is considered as standard reference.

In the experiments, the different methods including Binary, Otsu and Integer orders (v=1, 2) are used to compare with the new method, as shown in Fig.7.

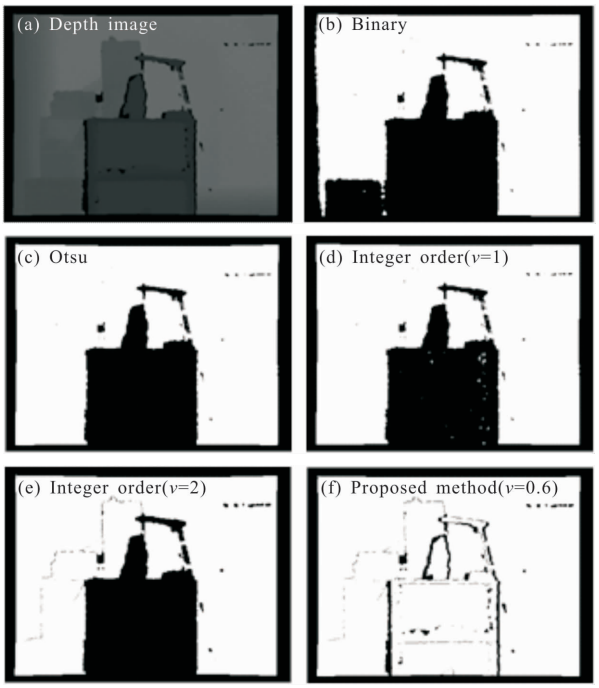

Fig.7 Comparison of different methods on shadow detection

The depth image from the Kinect sensor is shown in Fig.7(a), and the Fig.7(b) presents the result of the image binary with static threshold method, in which the threshold value is 47. As a typical adaptive threshold method, the Otsu method is applied in Fig.7(c). Compared with Binary method, the Otsu method can exclude the influence in left bottom. Unfortunately, they both consider the body arm and the backpack as the shadow, and the results are unacceptable.

Compared with the fractional differential, the integer differentials with first order and second order are shown in Fig.7(d) and Fig.7(e) respectively. In Fig.7(d), the boundary of the closet in the back is barely see, and it is clear to show the boundary in Fig.7(e). However, both of them still could not extract the body arm and the backpack as the shadow. At last, the proposed method can extract shadow region effectively as show in Fig.7(f).

The overall evaluation results of different methods are listed in Tab.1. It is obvious that our method can achieve the best result compared with other methods. For Recall, the compared four methods are with no obvious distinguished differences. The Recall of the edge detection on the first order and second order are 0.835 and 0.904 respectively, which present a little higher than that by Binary (0.761) and Otsu (0.792). The Recall of the proposed method is 0.937 which does not exhibit much better than that by other four methods. Although the other four methods have good references on Recall, they all over detected the shadow regions. Hence, our method is far beyond other four methods in Precision. The Otsu method is only 0.187 and the integer orders are just 0.372 and 0.473, while the proposed method is up to 0.908.

Tab.1 Evaluation results for different methods

Methods	Recall	Precision	F_1-score
Binary	0.761	0.148	0.248
Otsu	0.792	0.187	0.303
First order	0.835	0.372	0.515
Second order	0.904	0.473	0.621
Our method	0.937	0.908	0.918

For F_1-score, the new method can reach up to 0.918, while the others are all less than 0.65. Overall, the integer order has better result than that by other methods. Where the second order can obtain 0.621 on F_1-score, the Binary and Otsu are just 0.148 and 0.187. However, our method (0.6 order) can reach up to 0.918 which indicate the good performance of the fractional differential method on shadow detection.

In order to verify stability of the proposed method, plenty of depth images are selected to the experiment comparison on F_1-score. The Fig.8 illustrates the comparison of F_1-score values based on

related methods. Obviously, the Binary has the worst effect because its F_1−score values lie down the bottom of the figure. The second order exhibits better result than the first order and Otsu methods. Generally, the integer orders (first and second) have better performance than the Binary and Otsu methods, and the F_1−score values of these four methods are all less than 0.7. Moreover, the novel method can maintain the F_1−score values around 0.9, as shown in Tab.2.

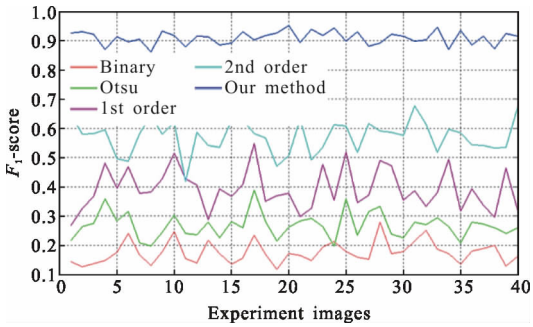

Fig.8 Comparison of different methods on shadow detection

Tab.2 F_1−score values of the related methods

Binary	Otsu	First order	Second order	Proposed method
0.145	0.218	0.268	0.646	0.925
0.126	0.264	0.326	0.580	0.930
0.137	0.276	0.367	0.583	0.921
0.148	0.359	0.481	0.596	0.870
0.177	0.284	0.396	0.496	0.913
0.240	0.316	0.468	0.488	0.895
0.168	0.209	0.379	0.582	0.904
0.131	0.197	0.383	0.644	0.862
0.178	0.245	0.428	0.581	0.932
0.248	0.303	0.515	0.621	0.918
…	…	…	…	…
0.214	0.279	0.386	0.676	0.897
0.252	0.270	0.332	0.615	0.903
0.187	0.295	0.380	0.517	0.945
0.173	0.264	0.494	0.597	0.869
0.136	0.209	0.319	0.584	0.934
0.181	0.279	0.393	0.544	0.886
0.189	0.273	0.338	0.541	0.916
0.199	0.260	0.297	0.533	0.872
0.129	0.241	0.464	0.536	0.923
0.164	0.261	0.319	0.675	0.916

Above all, the proposed method (blue line) stays the highest position in the figure, which indicates the best performance of the fractional differential method on shadow detection.

Moreover, the time cost of different methods are also test on Dell−Desktop with I5−CPU, 8G−RAM, Windows 7 −64 OS). The average time cost of different methods as shown in Tab.3. The average time cost of Binary and Otsu are a little less than the other methods. The proposed method exhibit almost same performance as the integer order methods.

Tab.3 Average time cost of related methods

Detection algorithms	Time cost/s
Binary	0.179
Otsu	0.201
First order	0.345
Second order	0.328
Our method	0.361

The experiments show that the proposed method has obvious superiority which can achieve the best F_1−score values. Consequently, compared with other traditional methods, the experiments verify that suggested method in this research can accomplish shadow detection effectively.

3 Conclusion

The research on Kinect sensor has attracted much attention in different application fields. Significant efforts have been made on ensure the depth image quality which is critical for Kinect sensor. However, the performance of most methods remains a challenge to accomplish satisfying results since the shadow noises. Therefore, this research is motivated by the need to develop a reasonable and trustful method for shadow detection on depth image processing. Accordingly, an improved operator based on fractional differential is studied to extract the shadow noises. The improved operator at 0.6 order can enhance the

boundaries of shadow regions significantly to accomplish the shadow detection effectively.

Experimental tests are conducted using a series of depth images collected by Kinect sensor, and the $F-$measure evaluation system is applied to verify the performance of the proposed method. Compared with other traditional methods, the F_1-score value of the novel method can reach up to 0.918, and the other methods are all less than 0.7. Hence, the results show that the proposed method has the ability to conduct satisfying result depth image processing.

The following are recommendations for future research:

(1) The quality of depth image has been significantly improved by using the proposed method. However, the current method still may not prove to handle tasks such as large-scale and outdoor depth images.

(2) Although depth image processing in this research can overcomes the influences of shadow noise, it is still a challenge to cope with complex objects and outdoor light situation. Therefore, it will be promising to develop related methods incorporating both color and depth image from Kinect sensor.

Acknowledgement

This research is financially supported by Key Research and Development Program in Shaanxi province of China (2019GY-038), and the Science and Technology Division Program in Xi′an of China (2017080CG/RC043(XALG017)).

References:

[1] Naeemabadi M Reza, Dinesen Birthe, Andersen Ole Kaeseler, et al. Influence of a Marker-based motion capture system on the performance of microsoft Kinect *v*2 skeleton algorithm [J]. ***IEEE Sensors Journal***, 2019, 19(1): 171-179.

[2] Zhao Min, Xiong Zhaolong, Xing Yan, et al. Real-time integral imaging pickup system based on binocular stereo camera [J]. ***Infrared and Laser Engineering***, 2017, 46(11): 1103007. (in Chinese)

[3] Guo Chunle, Li Chongyi, Guo Jichang, et al. Hierarchical features driven residual learning for depth map super-resolution[J]. ***IEEE Transaction on Image Processing***, 2019, 28(5): 2545-2557.

[4] Chen Guangda, Cui Guowei, Jin Zhongxiao, et al. Accurate intrinsic and extrinsic calibration of RGB-D cameras *w* with GP-based depth correction [J]. ***IEEE Sensors Journal,*** 2019, 19(7): 2685-2694.

[5] Cao Ting, Wang Weixing. Detection method for the depth of pavement broken block in cement concrete based on 3D laser scanning technology [J], ***Infrared and Laser Engineering***, 2017, 46(2): 0206006. (in Chinese)

[6] Moon Sungphill, Park Youngbin, Ko Dong Wook, et al. Multiple kinect sensor fusion for human skeleton tracking using Kalman filtering [J]. ***International Journal of Advanced Robotic Systems***, 2016, 13(65): 1-10.

[7] Boutellaa Elhocine, Hadid Abdenour, Bengherabi Messaoud, et al. On the use of Kinect depth data for identity, gender and ethnicity classification from facial images [J]. ***Pattern Recognition Letters***, 2015, 68(2): 270-277.

[8] Hu Jinhui, Hu Ruimin, Wang Zhongyuan, et al. Color image guided locality regularized representation for depth holes filling [C]//IEEE International Conference on Visual Communications and Image Processing (VCIP), 2013: 17-20.

[9] Yang Jingyu, Gan Ziqiao, Li Kun, et al. Graph-based segmentation for RGB-D data using 3-D geometry enhanced superpixels [J]. ***IEEE Trans Cybern***, 2015, 45(5): 913-926.

[10] Camplani Massimo, Salgado Luis. Efficient spatio-temporal hole filling strategy for Kinect depth maps [C]//Three-Dimensional Image Processing (3DIP) and Applications, 2012: 8290.

[11] Maimone Andrew, Bidwell Jonathan, Peng Kun, et al. Enhanced personal auto stereoscopic telepresence system using commodity depth cameras [J]. ***Comput Graph***, 2012, 36(7): 791-807.

[12] Essmaeel Kyis, Gallo Luigi, Damiani Ernesto, et al. Comparative evaluation of methods for filtering Kinect depth data[J]. ***Multimed Tools Appl***, 2015, 74(17): 7331-7354.

[13] Deng Teng, Li Hui, Cai Jianfei, et al. Kinect shadow detection and classification[C]//IEEE International Conference on Computer Vision Workshops, 2013: 708-713.

[14] Ma Ronggui, Cao Ting, Wang Weixing. HUD image vibration detection on improved edge detection and corner extraction [J] ***International Journal of Signal Processing,*** 2014, 7(1): 393-404.

[15] Pu Yifei, Zhou Jiliu, Yuan Xiao. Fractional differential mask: a fractional differential-based approach for milti scale texture enhancement [J]. ***IEEE Transactions on Image Processing***, 2010, 19(2): 491-511.

[16] Perrin Emmanuel, Harba Rachid, Corinne Berzin-Joseph, et al. *n*th-order fractional Brownian motion and fractional Gaussian noises [J]. ***IEEE Transactions on Signal Processing***, 2001, 49(5): 1049-1059.

[17] Hu Fuyuan, Si Shaohui, San Wong, et al. An adaptive approach for texture enhancement based on a fractional differential operator with non-integer step and order [J]. ***Neurocomputing***, 2015, 158: 295-306.

[18] Cao Ting, Wang Weixing, Tighe Susan, et al. Crack image detection based on fractional differential and fractal dimension [J]. ***IET Computer Vision***, 2019, 13(1): 79-58.

[19] Li Bo, Xie Lei. Image denoising and enhancement based on adaptive fractional calculus of small probability strategy [J]. ***Neurocomputing***, 2016, 175: 704-717.

[20] Cao Ting, Yang Nan, Wang Fengping, et al. Crack image segmentation based on improved DBC method [C]//SPIE Conference on LIDAR Imaging Detection and Target Recognition, 2017, 15(11): 106052B.